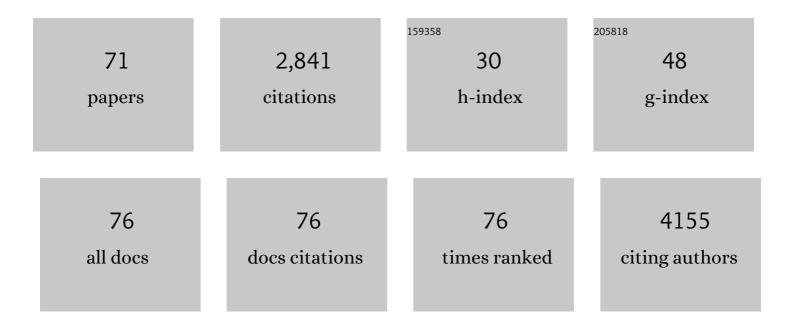
Christopher M Haggerty

List of Publications by Year in descending order

Source: https://exaly.com/author-pdf/3940910/publications.pdf Version: 2024-02-01



#	Article	IF	CITATIONS
1	Genome-wide association and Mendelian randomisation analysis provide insights into the pathogenesis of heart failure. Nature Communications, 2020, 11, 163.	5.8	466
2	Prediction of mortality from 12-lead electrocardiogram voltage data using a deep neural network. Nature Medicine, 2020, 26, 886-891.	15.2	168
3	Routinely reported ejection fraction and mortality in clinical practice: where does the nadir of risk lie?. European Heart Journal, 2020, 41, 1249-1257.	1.0	167
4	Association Between Titin Loss-of-Function Variants and Early-Onset Atrial Fibrillation. JAMA - Journal of the American Medical Association, 2018, 320, 2354.	3.8	144
5	Deep Neural Networks Can Predict New-Onset Atrial Fibrillation From the 12-Lead ECG and Help Identify Those at Risk of Atrial Fibrillation–Related Stroke. Circulation, 2021, 143, 1287-1298.	1.6	134
6	Predicting Survival From LargeÂEchocardiography and ElectronicÂHealthÂRecord Datasets. JACC: Cardiovascular Imaging, 2019, 12, 681-689.	2.3	101
7	Genomics-First Evaluation of Heart Disease Associated With Titin-Truncating Variants. Circulation, 2019, 140, 42-54.	1.6	97
8	Fontan hemodynamics from 100 patient-specific cardiac magnetic resonance studies: A computational fluid dynamics analysis. Journal of Thoracic and Cardiovascular Surgery, 2014, 148, 1481-1489.	0.4	86
9	Analysis of rare genetic variation underlying cardiometabolic diseases and traits among 200,000 individuals in the UK Biobank. Nature Genetics, 2022, 54, 240-250.	9.4	68
10	Cardiac remodeling and dysfunction in childhood obesity: a cardiovascular magnetic resonance study. Journal of Cardiovascular Magnetic Resonance, 2016, 18, 28.	1.6	62
11	Smooth Muscle Cell Deletion of Low-Density Lipoprotein Receptor–Related Protein 1 Augments Angiotensin Il–Induced Superior Mesenteric Arterial and Ascending Aortic Aneurysms. Arteriosclerosis, Thrombosis, and Vascular Biology, 2015, 35, 155-162.	1.1	60
12	Geometric Characterization of Patient-Specific Total Cavopulmonary Connections and its Relationship to Hemodynamics. JACC: Cardiovascular Imaging, 2014, 7, 215-224.	2.3	59
13	Experimental and numeric investigation of Impella pumps as cavopulmonary assistance for a failing Fontan. Journal of Thoracic and Cardiovascular Surgery, 2012, 144, 563-569.	0.4	53
14	Comparing Pre- and Post-operative Fontan Hemodynamic Simulations: Implications for the Reliability of Surgical Planning. Annals of Biomedical Engineering, 2012, 40, 2639-2651.	1.3	52
15	Individualized computer-based surgical planning to address pulmonary arteriovenous malformations in patients with a single ventricle with an interrupted inferior vena cava and azygous continuation. Journal of Thoracic and Cardiovascular Surgery, 2011, 141, 1170-1177.	0.4	48
16	Numerical, Hydraulic, and Hemolytic Evaluation of an Intravascular Axial Flow Blood Pump to Mechanically Support Fontan Patients. Annals of Biomedical Engineering, 2011, 39, 324-336.	1.3	47
17	Visualization of flow structures in Fontan patients using 3-dimensional phase contrast magnetic resonance imaging. Journal of Thoracic and Cardiovascular Surgery, 2012, 143, 1108-1116.	0.4	45
18	Hemodynamic Modeling of Surgically Repaired Coarctation of the Aorta. Cardiovascular Engineering and Technology, 2011, 2, 288-295.	0.7	44

#	Article	IF	CITATIONS
19	A Machine Learning Approach to Management of HeartÂFailure Populations. JACC: Heart Failure, 2020, 8, 578-587.	1.9	44
20	Electronic health record phenotype in subjects with genetic variants associated with arrhythmogenic right ventricular cardiomyopathy: a study of 30,716 subjects with exome sequencing. Genetics in Medicine, 2017, 19, 1245-1252.	1.1	43
21	Preliminary clinical experience with a bifurcated Y-graft Fontan procedure—A feasibility study. Journal of Thoracic and Cardiovascular Surgery, 2012, 144, 383-389.	0.4	42
22	Prevalence and Electronic Health Record-Based Phenotype of Loss-of-Function Genetic Variants in Arrhythmogenic Right Ventricular Cardiomyopathy-Associated Genes. Circulation Genomic and Precision Medicine, 2019, 12, e002579.	1.6	42
23	A genome-first approach to aggregating rare genetic variants in LMNA for association with electronic health record phenotypes. Genetics in Medicine, 2020, 22, 102-111.	1.1	42
24	Simulating hemodynamics of the Fontan Y-graft based on patient-specific inÂvivo connections. Journal of Thoracic and Cardiovascular Surgery, 2013, 145, 663-670.	0.4	39
25	Patients with repaired tetralogy of Fallot suffer from intra- and inter-ventricular cardiac dyssynchrony: a cardiac magnetic resonance study. European Heart Journal Cardiovascular Imaging, 2014, 15, 1333-1343.	0.5	36
26	Left and right ventricular dyssynchrony and strains from cardiovascular magnetic resonance feature tracking do not predict deterioration of ventricular function in patients with repaired tetralogy of Fallot. Journal of Cardiovascular Magnetic Resonance, 2016, 18, 49.	1.6	36
27	Energetic Implications of Vessel Growth and Flow Changes Over Time in Fontan Patients. Annals of Thoracic Surgery, 2015, 99, 163-170.	0.7	35
28	Fontan Pathway Growth: A Quantitative Evaluation of Lateral Tunnel and Extracardiac Cavopulmonary Connections Using Serial Cardiac Magnetic Resonance. Annals of Thoracic Surgery, 2014, 97, 916-922.	0.7	32
29	Reproducibility of cine displacement encoding with stimulated echoes (DENSE) cardiovascular magnetic resonance for measuring left ventricular strains, torsion, and synchrony in mice. Journal of Cardiovascular Magnetic Resonance, 2013, 15, 71.	1.6	31
30	Obesity reduces left ventricular strains, torsion, and synchrony in mouse models: a cine displacement encoding with stimulated echoes (DENSE) cardiovascular magnetic resonance study. Journal of Cardiovascular Magnetic Resonance, 2013, 15, 109.	1.6	30
31	Can time-averaged flow boundary conditions be used to meet the clinical timeline for Fontan surgical planning?. Journal of Biomechanics, 2017, 50, 172-179.	0.9	29
32	Association between left ventricular mechanics and diffuse myocardial fibrosis in patients with repaired Tetralogy of Fallot: a cross-sectional study. Journal of Cardiovascular Magnetic Resonance, 2017, 19, 100.	1.6	29
33	Deep-learning-assisted analysis of echocardiographic videos improves predictions of all-cause mortality. Nature Biomedical Engineering, 2021, 5, 546-554.	11.6	29
34	Comparison of left ventricular strains and torsion derived from feature tracking and DENSE CMR. Journal of Cardiovascular Magnetic Resonance, 2018, 20, 63.	1.6	28
35	Validation of in vivo 2D displacements from spiral cine DENSE at 3T. Journal of Cardiovascular Magnetic Resonance, 2015, 17, 5.	1.6	24
36	Right Ventricular Strain, Torsion, and Dyssynchrony in Healthy Subjects Using 3D Spiral Cine DENSE Magnetic Resonance Imaging. IEEE Transactions on Medical Imaging, 2017, 36, 1076-1085.	5.4	23

#	Article	IF	CITATIONS
37	rECHOmmend: An ECG-Based Machine Learning Approach for Identifying Patients at Increased Risk of Undiagnosed Structural Heart Disease Detectable by Echocardiography. Circulation, 2022, 146, 36-47.	1.6	21
38	Relationship of Single Ventricle Filling and Preload to Total Cavopulmonary Connection Hemodynamics. Annals of Thoracic Surgery, 2015, 99, 911-917.	0.7	20
39	SURGEM: A solid modeling tool for planning and optimizing pediatric heart surgeries. CAD Computer Aided Design, 2016, 70, 3-12.	1.4	20
40	Treatment planning for a TCPC test case: A numerical investigation under rigid and moving wall assumptions. International Journal for Numerical Methods in Biomedical Engineering, 2013, 29, 197-216.	1.0	19
41	Telemetric Blood Pressure Assessment in Angiotensin II-Infused ApoE-/- Mice: 28 Day Natural History and Comparison to Tail-Cuff Measurements. PLoS ONE, 2015, 10, e0130723.	1.1	16
42	Numerical and experimental investigation of pulsatile hemodynamics in the total cavopulmonary connection. Journal of Biomechanics, 2013, 46, 373-382.	0.9	15
43	Simplified post processing of cine DENSE cardiovascular magnetic resonance for quantification of cardiac mechanics. Journal of Cardiovascular Magnetic Resonance, 2014, 16, 94.	1.6	15
44	Clinical Findings and Diagnostic Yield of Arrhythmogenic Cardiomyopathy Through Genomic Screening of Pathogenic or Likely Pathogenic Desmosome Gene Variants. Circulation Genomic and Precision Medicine, 2021, 14, e003302.	1.6	14
45	Monogenic and Polygenic Contributions to QTc Prolongation in the Population. Circulation, 2022, 145, 1524-1533.	1.6	14
46	The genetic architecture of Plakophilin 2 cardiomyopathy. Genetics in Medicine, 2021, 23, 1961-1968.	1.1	13
47	Laser Flow Measurements in an Idealized Total Cavopulmonary Connection With Mechanical Circulatory Assistance. Artificial Organs, 2011, 35, 1052-1064.	1.0	12
48	Managing Secondary Genomic Findings Associated With Arrhythmogenic Right Ventricular Cardiomyopathy. Circulation Genomic and Precision Medicine, 2018, 11, e002237.	1.6	11
49	Haemodynamic comparison of a novel flow-divider Optiflo geometry and a traditional total cavopulmonary connection. Interactive Cardiovascular and Thoracic Surgery, 2013, 17, 1-7.	0.5	10
50	Quantification of left ventricular volumes, mass, and ejection fraction using cine displacement encoding with stimulated echoes (DENSE) MRI. Journal of Magnetic Resonance Imaging, 2014, 40, 398-406.	1.9	10
51	Left ventricular mechanical dysfunction in diet-induced obese mice is exacerbated during inotropic stress: a cine DENSE cardiovascular magnetic resonance study. Journal of Cardiovascular Magnetic Resonance, 2015, 17, 75.	1.6	10
52	Hemodynamic Impact of Superior Vena Cava Placement in the Y-Graft Fontan Connection. Annals of Thoracic Surgery, 2016, 101, 183-189.	0.7	10
53	Uniquely shaped cardiovascular stents enhance the pressure generation of intravascular blood pumps. Journal of Thoracic and Cardiovascular Surgery, 2012, 144, 704-709.	0.4	9
54	2D cine DENSE with low encoding frequencies accurately quantifies cardiac mechanics with improved image characteristics. Journal of Cardiovascular Magnetic Resonance, 2015, 17, 93.	1.6	9

#	Article	IF	CITATIONS
55	An interactive videogame designed to improve respiratory navigator efficiency in children undergoing cardiovascular magnetic resonance. Journal of Cardiovascular Magnetic Resonance, 2016, 18, 54.	1.6	9
56	Genetic counseling for patients with positive genomic screening results: Considerations for when the genetic test comes first. Journal of Genetic Counseling, 2021, 30, 634-644.	0.9	9
57	Left ventricular and atrial segmentation of 2D echocardiography with convolutional neural networks. , 2020, , .		9
58	Loss-of-Function <i>FLNC</i> Variants Are Associated With Arrhythmogenic Cardiomyopathy Phenotypes When Identified Through Exome Sequencing of a General Clinical Population. Circulation Genomic and Precision Medicine, 2022, 15, .	1.6	8
59	Rare Coding Variants Associated With Electrocardiographic Intervals Identify Monogenic Arrhythmia Susceptibility Genes: A Multi-Ancestry Analysis. Circulation Genomic and Precision Medicine, 2021, 14, e003300.	1.6	7
60	Of mice (dogs) and men: getting to the heart of obesity-associated cardiac dysfunction. Diabetologia, 2016, 59, 9-12.	2.9	4
61	Assessing the generalizability of temporally coherent echocardiography video segmentation. , 2021, , .		4
62	3D-Encoded DENSE MRI with Zonal Excitation for Quantifying Biventricular Myocardial Strain During a Breath-Hold. Cardiovascular Engineering and Technology, 2021, , 1.	0.7	4
63	Genomic Screening for Pathogenic Transthyretin Variants Finds Evidence of Underdiagnosed Amyloid Cardiomyopathy From Health Records. JACC: CardioOncology, 2021, 3, 550-561.	1.7	4
64	Generalizability and quality control of deep learning-based 2D echocardiography segmentation models in a large clinical dataset. International Journal of Cardiovascular Imaging, 2022, 38, 1685-1697.	0.7	4
65	Using a respiratory navigator significantly reduces variability when quantifying left ventricular torsion with cardiovascular magnetic resonance. Journal of Cardiovascular Magnetic Resonance, 2017, 19, 25.	1.6	3
66	Rad GTPase Deletion Attenuates Post-Ischemic Cardiac Dysfunction andÂRemodeling. JACC Basic To Translational Science, 2018, 3, 83-96.	1.9	3
67	Magnetic resonance imaging-guided surgical design: can we optimise the Fontan operation?. Cardiology in the Young, 2013, 23, 818-823.	0.4	2
68	Optimal configuration of respiratory navigator gating for the quantification of left ventricular strain using spiral cine displacement encoding with stimulated echoes (DENSE) MRI. Journal of Magnetic Resonance Imaging, 2017, 45, 786-794.	1.9	2
69	Typical readout durations in spiral cine DENSE yield blurred images and underestimate cardiac strains at both 3.0â€⊤ and 1.5â€⊤. Magnetic Resonance Imaging, 2018, 54, 90-100.	1.0	2
70	Pulsatile Hemodynamics of the Fontan Connection: A Tri-Modal Investigation. , 2011, , .		1
71	High resolution cine displacement encoding with stimulated echoes (DENSE) at 3T with navigator feedback for quantification of cardiac mechanics. Journal of Cardiovascular Magnetic Resonance, 2014, 16, P48.	1.6	1